Bulletin of the Seismological Society of America, Vol. 97, No. 4, pp. 1259–1266, August 2007, doi: 10.1785/0120060171

Q of Lg Waves in the Central Mexican Volcanic Belt

by S. K. Singh, A. Iglesias, D. García, J. F. Pacheco, and M. Ordaz

Abstract From seismograms of nine shallow, coastal earthquakes recorded at a pair of broadband stations, we estimate Q of Lg waves in the part of central Mexican Volcanic Belt (MVB) that includes the Valley of Mexico. The two stations straddle the central MVB and are located on Cretaceous limestone. A weighted least-square fit to the $Q^{-1}(f)$ data in the frequency range 0.25 to 8 Hz yields $Q(f) = 98f^{0.72}$. This estimate of Q is lower than the corresponding Q in the forearc region that is given by $Q(f) = 273f^{0.66}$. Note that our estimate of $Q(f)$ corresponds to a 200-km-wide zone of the MVB. The result of this study sheds light on the characteristics of seismic waves as they traverse through the MVB where they undergo dramatic amplification in the Valley of Mexico. It also provides one of the critical elements needed in the estimation of expected ground motions at sites to the north of the MVB from future coastal earthquakes. The lower Q of Lg waves in the MVB as compared with the forearc region seems correlated with lower resistivity reported in the MVB relative to the forearc region.

Introduction

Present-day tectonics of central Mexico is related to the subduction of oceanic Rivera and Cocos plates below the continent. This process gives rise to interplate and inslab seismicity. Although in general it is thought that the origin of the Mexican Volcanic Belt (MVB) is related to the subduction of the oceanic plates, this is not universally accepted (see Verma [2002] and Ferrari [2004] for opposite points of view). The MVB is subparallel to the middle America trench (Fig. 1). The central part of the MVB, which includes the Valley of Mexico, is about 200 km wide (Fig. 1) and comprises rocks of Pliocene and Quaternary age (Demant, 1981; Robin, 1981). The present volcanic activity is confined to the southern part of the central MVB. The seismicity in the subducted oceanic plate ceases to the south of the MVB (near PLIG in Fig. 1) at a depth of about 50 km. In fact, the lack of inslab seismicity below the MVB and unusual geochemical signature of some of the volcanic rocks in the region are the main reasons to seek alternative models for the origin of the MVB that are not related to the subduction of the ocean slab.

The MVB plays a critical role in the nature of ground motions recorded in the Valley of Mexico. For example, it is well known that the seismic waves propagating from the Pacific coast of Mexico toward the Valley of Mexico (Fig. 1) get amplified in the MVB (e.g., Singh *et al.*, 1988b; Ordaz and Singh, 1992). They suffer further and dramatic amplification in the lake-bed zone of the valley (Singh *et al.*, 1988a,b), which is the principal cause of damage to Mexico City during large, coastal earthquakes. This phenomenon has been well documented since 1985 when strong-motion stations became operational along the Pacific coast of Mexico, along an attenuation line extending from the coast to Mexico City and in the city itself. Numerous studies have quantified and modeled the amplification of seismic waves in the MVB. Although the seismic intensities are known to diminish rapidly to the north of the Valley of Mexico (e.g., Figueroa, 1987), the characteristics of the seismic waves after they cross the MVB have not been studied quantitatively. This is mainly due to the lack of permanent seismographs to the north of MVB. Until late 2003, seismic recordings at the northern end of the central MVB were limited to those obtained from portable seismographs. In 1994 a portable network of nine broadband stations was operated for about two months along a line crossing the MVB in the region of the Valley of Mexico (Shapiro *et al.*, 1997). The goal was to study surface-wave propagation and mapping of shallow crustal structure of the region. Although the study demonstrated a correlation between the superficial low-velocity layer and seismic-wave amplification, it did not quantify attenuation of seismic waves across MVB except at long periods (8–10 sec). Thus, the role of the MVB on the spectral amplitudes to the north of the MVB still remains poorly understood.

Clearly, knowledge of Q of the MVB could provide an understanding of the seismic waves after they traverse the MVB. Furthermore, a reliable estimate of Q would give important clues to the physical conditions of the MVB. Unfortunately, as we summarize in the following, the current literature gives inconsistent estimates of Q of the MVB.

Canas (1986) studied coda Q of Lg waves in the MVB and reported $Q(f) = 332f^{0.4}$ and $Q(f) = 129f^{0.6}$ for the

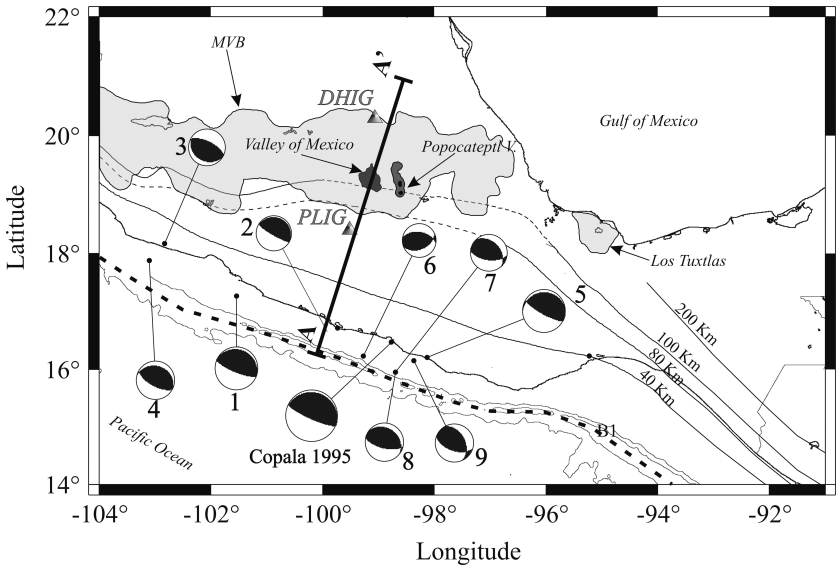

Figure 1. Map of the region showing locations and focal mechanisms of the earthquakes analyzed in this study. Gray zone delineates the MVB. Los Tuxtlas define the eastern limit of the MVB. Isodepth contours of the Benioff zone are marked (dashed where inferred). Seismograms at stations PLIG and DHIG are used to estimate Q of Lg waves of the central MVB. A cross section along AA′ is shown in Figure 7.

central and eastern part of the volcanic belt, respectively. In Canas' study, both the seismograph and the sources were located in the volcanic belt. Yamamoto *et al.* (1997) analyzed coda of Lg waves recorded on a broadband seismograph located in the Valley of Mexico. These authors reported $Q(f) \sim 335f^{0.9}$ for the eastern volcanic belt and suggested that the apparent high Q might in part be a consequence of wave-guide effect. Shapiro *et al.* (2000) noted anomalously high attenuation of S waves crossing the presently active Popocatepetl volcano (Fig. 1) and estimated Q of S wave below the volcano as ~60 (2–6 Hz). Ottemöller *et al.* (2002) performed a tomographic study of Q of Lg waves in southern Mexico and obtained $Q(f) = 238f^{0.486}$ (1–6 Hz) for the MVB near the Valley of Mexico. Ortega *et al.* (2003) analyzed data recorded by 13 stations located in the MVB in and around the Valley of Mexico City (11 equipped with short-period seismographs and two with broadband seismographs), and reported $Q(f) = 180f^{0.66}$. Ortega and Quintanar (2005) augmented the dataset used in Ortega *et al.* (2003) with more recent events from the Valley of Mexico, eliminated others (R. Ortega, personal communication, 2007), and obtained $Q = 110f^{0.66}$ in the MVB based on consistent comparison of local magnitude and ground-motion scaling.

The large variability in the reported Q of the MVB reflects the difference in the source characteristics and location of earthquakes, and the data and methodology used in the analysis. We note that the estimations of Q based on recordings within the MVB are likely to be contaminated by amplification of seismic waves caused by shallow, surface layers of low velocity (Singh *et al.*, 1995). The simplest way to obtain reliable estimates of average Q of Lg waves of the central MVB is to use recordings at stations situated on hard sites that straddle the MVB. It is this strategy that we pursue in this study.

In December 2003 a permanent broadband seismograph became operational at DHIG at the north end of the MVB. In this study we analyze seismograms of nine shallow, coastal, thrust events recorded at the pair of broadband stations DHIG and PLIG (Fig. 1, Table 1). The stations, which are 217 km apart, straddle the central MVB: PLIG to the south and DHIG to the north. Both are located on Cretaceous limestone. The average ratio of horizontal to vertical spectral amplitudes at these stations is close to 1 (Fig. 2), suggesting negligible site effect. From Lg-wave spectra at DHIG and PLIG, we estimate Q of the MVB and compare it with that of the forearc region. We finally discuss implications of our results in earthquake engineering and its relation with the present tectonics of the region.

Data and Analysis

The nine events listed in Table 1 are the only shallow, coastal earthquakes that have been recorded so far by both DHIG and PLIG with reliable spectra in the bandwidth of 0.25–8 Hz. The seismographs consist of 24-bit Quanterra digitizers connected to STS-2 sensors. The data, recorded at

Table 1
Earthquakes Analyzed in This Study*

Event No.	Date	Latitude (° N)	Longitude (° W)	H (km)	M_W	Strike ϕ^0	Dip δ^0	Rake λ^0
1	1 Jan. 2004	17.27	101.54	17	6.0†	299	13	92
2	4 Jan. 2004	16.69	99.71	10	4.8‡	295	8	85
3	6 Feb. 2004	18.16	102.83	35	5.1†	296	65	88
4	21 May 2004	17.87	103.11	28	5.2†	287	24	79
5	14 Jun. 2004	16.19	98.13	20	5.9†	277	11	70
6	28 Sep. 2004	16.22	99.25	23	4.6‡	276	50	112
7	15 Nov. 2004	16.00	98.74	18	5.3†	295	21	94
8	15 Nov. 2004	15.96	98.47	19	5.1†	306	26	110
9	14 Aug. 2005	16.14	98.35	12	5.4†	278	16	61

*All locations are based on local/regional data with the exception of events 3 and 4 whose depths are taken from the Harvard CMT catalog.
†M_W and focal mechanism from Harvard CMT catalog.
‡M_W and focal mechanism from regional moment tensor inversion.

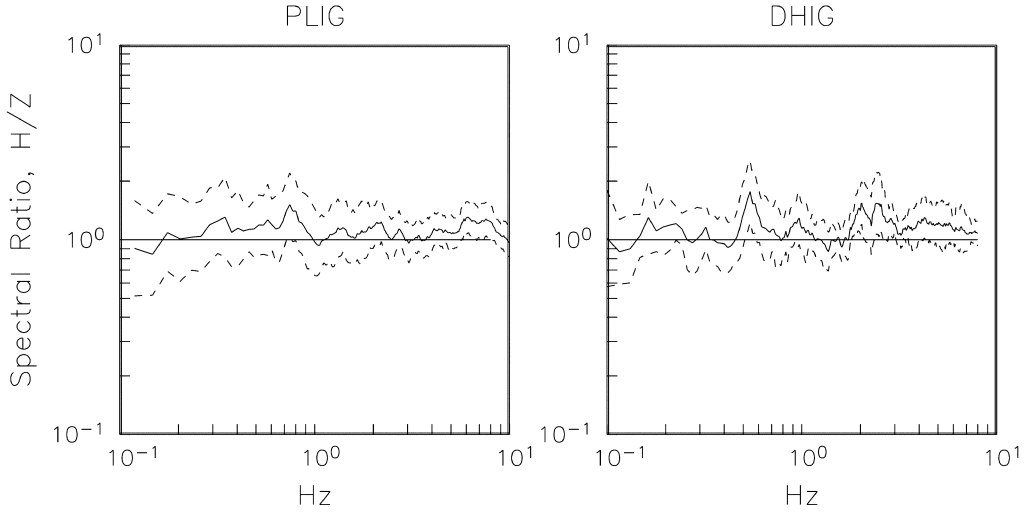

Figure 2. Horizontal-to-vertical spectral ratios of *Lg* wave at PLIG and DHIG as function of frequency. Median and ± one standard deviation curves are also shown.

80 samples/sec, were corrected for instrumental response and converted to ground acceleration. The time window used in the analysis began with *S*-wave arrival and included 95% of the total energy. The signals were Fourier transformed by an FFT routine, smoothed by a 1/6 octave-band filter, and 5% tapered. The spectral amplitudes were measured at 11 frequencies equally spaced in logarithmic domain between 0.25 and 8 Hz.

Let $Sd(f)$ and $Sp(f)$ be the acceleration spectral amplitudes of *Lg* waves of an earthquake at DHIG and PLIG, respectively, and let *Rd* and *Rp* be the corresponding hypocentral distances to these stations. Since the great circle path from the epicenter to DHIG does not, in general, pass through PLIG, we reduced the spectral amplitudes at PLIG to a distance *Rm* which is the distance from the epicenter to the southernmost point of the MVB along the great circle path to DHIG. Note that *Rm* is different for each event. Let this amplitude be $Sm(f)$ which may be written as:

$$Sm(f) = Sp(f)(Rp/Rm)^{1/2}\, e^{-\pi f(Rm-Rp)/UQ_{\text{in}}(f)} \qquad (1)$$

where U is the group velocity of *Lg* waves (taken here as 3.5 km/sec) and $Q_{\text{in}}(f)$ is the quality factor of *Lg* waves in the forearc region, between the coast and the inland stations south of the MVB. Following Ordaz and Singh (1992) we take $Q_{\text{in}}(f) = 273f^{0.66}$. In equation (1) we are assuming that the geometrical spreading of *Lg* waves is adequately described by $1/R^{1/2}$ for R greater than about 150 km. This is supported by previous results (e.g., Ordaz and Singh, 1992; Ortega *et al.*, 2003) and elsewhere. Similar to equation (1) we may write:

$$[Sd(f)/Sm(f)] = (Rm/Rd)^{1/2}\, e^{-\pi f(Rd-Rm)/UQ(f)}. \qquad (2)$$

From equations (2) and (1),

$$[Sd(f)/Sp(f)] = (Rp/Rd)^{1/2}\, e^{-\pi f/U[\{(Rm-Rp)/Q_{\text{in}}(f)\}+\{(Rd-Rm)/Q(f)\}]} \qquad (3)$$

where $Q(f)$ is the quality factor of *Lg* waves in the MVB. We take logarithms of both sides of equation (3) and obtain $Q^{-1}(f)$ at each selected frequency for each event. $Q^{-1}(f)$ was computed for the cuadratic mean of the spectral amplitudes of the two horizontal components and the vertical component separately.

Figure 3 illustrates the analysis for event 5 (Table 1). In this case, $Rd = 464$ km, $Rp = 285$ km, and $Rm = 245$ km. The figure shows observed spectral amplitudes $Sp(f)$ and $Sd(f)$ at PLIG and DHIG, respectively, and the computed amplitude $Sm(f)$ at the southern most point of the MVB along the great circle path from the epicenter to DHIG. Because *Rp* roughly equals *Rm, Sp*(*f*) also approximately equals $Sm(f)$. If we assume the $Q(f) = Q_{\text{in}}(f) = 273f^{0.66}$ then the predicted spectral amplitudes at DHIG are much greater than the observed ones, which strongly indicates that that the Q of *Lg* waves in the MVB is smaller than in the forearc region (between the coast and the MVB).

Results

$Q^{-1}(f)$

Figure 4 shows $Q^{-1}(f)$ obtained from the analysis of the nine events. One of the 198 values of $Q^{-1}(f)$ (9 events, 11 frequencies, horizontal and vertical components) was negative at 0.5 Hz. This value was excluded from the analysis. The results corresponding to horizontal, vertical, and both horizontal and vertical components are shown in the left, central, and right frames, respectively. The bottom frames plot $Q^{-1}(f)$ for each event at each selected frequency, whereas the top frames show the mean value and ± one standard deviation of $Q^{-1}(f)$. As seen in the top left and

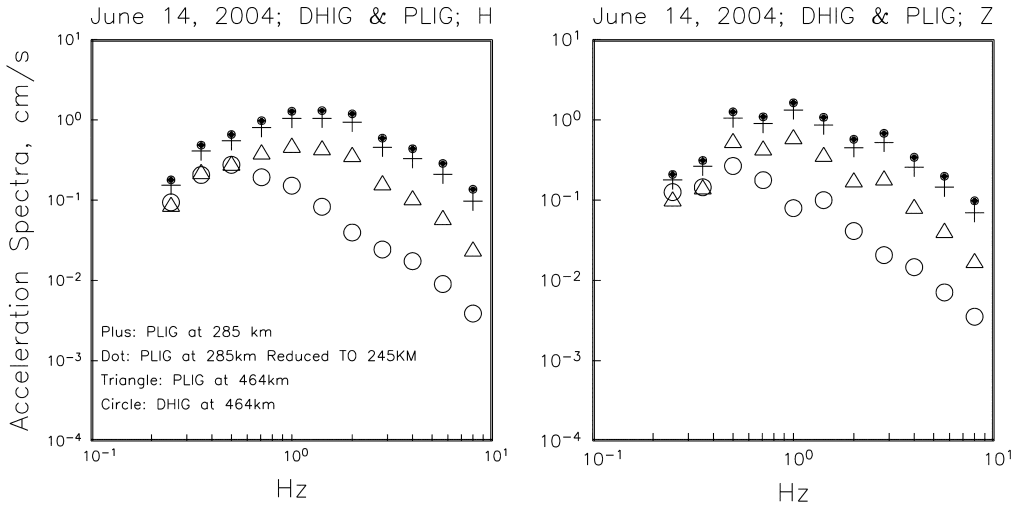

Figure 3. Observed spectral amplitudes at PLIG (plusses) and DHIG (circles), and computed amplitudes at the southern most point of the MVB along the great circle path from the epicenter to DHIG for event 5. Because *Rp* roughly equals *Rm, Sp*(*f*) also approximately equals *Sm*(*f*). The predicted spectral amplitudes at DHIG (triangles) are much greater than the observed ones if *Q* of *Lg* waves in the MVB is taken to be the same as that for the forearc region reported by Ordaz and Singh (1992).

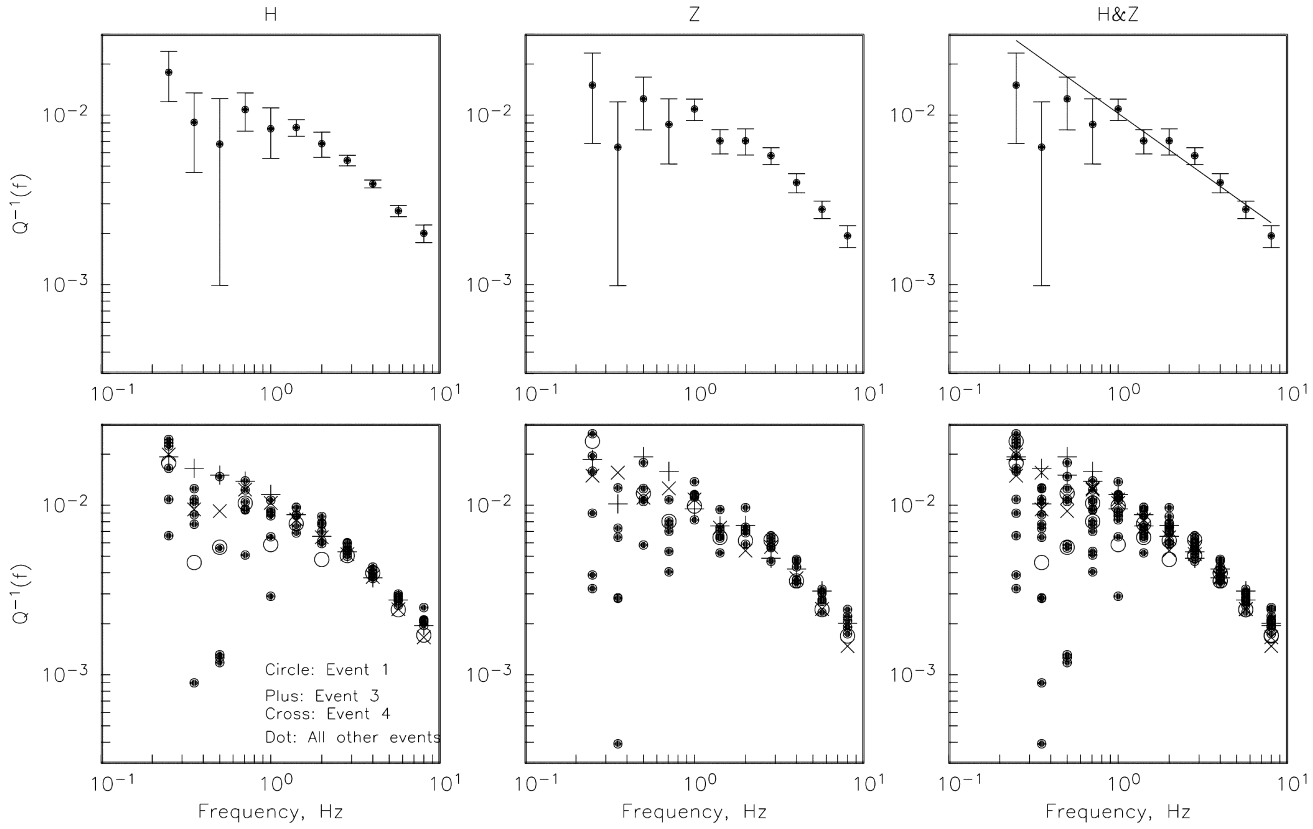

Figure 4. $Q^{-1}(f)$ of MVB as a function of frequency. Bottom frames: $Q^{-1}(f)$ for each event at each selected frequency. Top frames: mean and ± one standard deviation of $Q^{-1}(f)$. Left, central, and right frames correspond to horizontal, vertical, and horizontal plus vertical components, respectively. The straight line in the upper right frame is a weighted least-square fit to the data (equation 4).

central frames, the horizontal and vertical components yield similar values of $Q^{-1}(f)$. We note that there is large uncertainty in $Q^{-1}(f)$ at low frequencies ($f \leq 0.5$ Hz). Similar large uncertainties in $Q^{-1}(f)$ at low frequencies have been reported in the tomographic study of *Lg* waves of Mexican earthquakes by Ottemöller *et al.* (2002) and in the study of *S* waves from inslab Mexican earthquakes by Garcia *et al.* (2004).

The plots in Figure 4 show that a simple functional form of the type $Q^{-1}(f) = \alpha f^{\beta}$ does not adequately describe the data over the entire frequency range. If, however, the data are fit to this functional form, then a weighted least-squares fit, including both the horizontal and vertical spectral amplitude data, yields

$$Q^{-1}(f) = (0.01024 \pm 0.00066)\, f^{-(0.717 \pm 0.050)} \qquad (4)$$

or, $Q(f) = 98.6f^{0.72}$. This fit is shown in the right top frame of Figure 4. We note that $Q^{-1}(f)$ obtained in this study is an average for the 200-km-wide zone of the central MVB. The southern part of the MVB, with its present volcanic activity, may have a much lower Q.

Our estimate of $Q^{-1}(f)$ is based on the following three assumptions. (1) Stations PLIG and DHIG are free of site effect. This is supported by (H/Z) spectral ratio and the fact that the stations are located on hard limestone formations. (2) Q of *Lg* waves between the coast and the inland stations south of the MVB (the forearc region) is accurately given by $Q_{in}(f) = 273f^{0.66}$. We note that an error in $Q_{in}(f)$, however, would not cause appreciable error in $Q^{-1}(f)$ for six of the nine events since, for these events, *Rp* roughly equals *Rm*. For events 1, 3, and 4, *Rm* does differ substantially from *Rp* (Fig. 1). Nevertheless, $Q^{-1}(f)$ values for these events are close to the rest of the events (Fig. 4). This suggests that $Q_{in}(f) = 273f^{0.66}$ is reasonably accurate. (3) The geometrical spreading between PLIG and DHIG is adequately de-

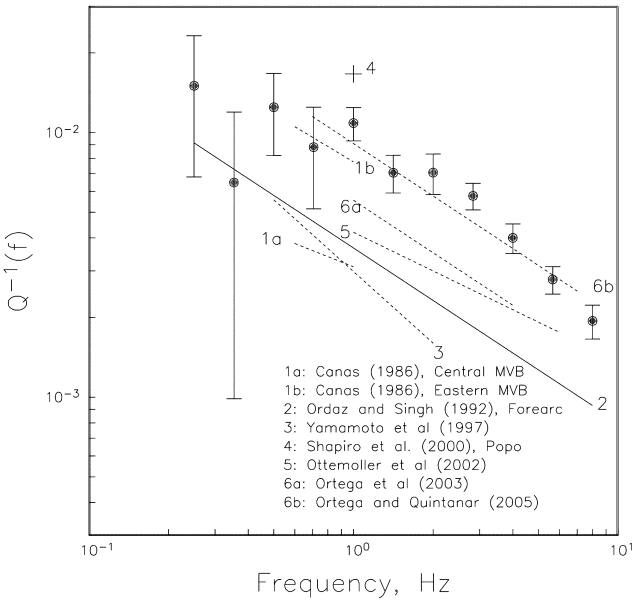

Figure 5. $Q^{-1}(f)$ of MVB obtained in this study (dots) and those reported in previous works. Also shown is $Q^{-1}(f)$ of Lg waves in the forearc region.

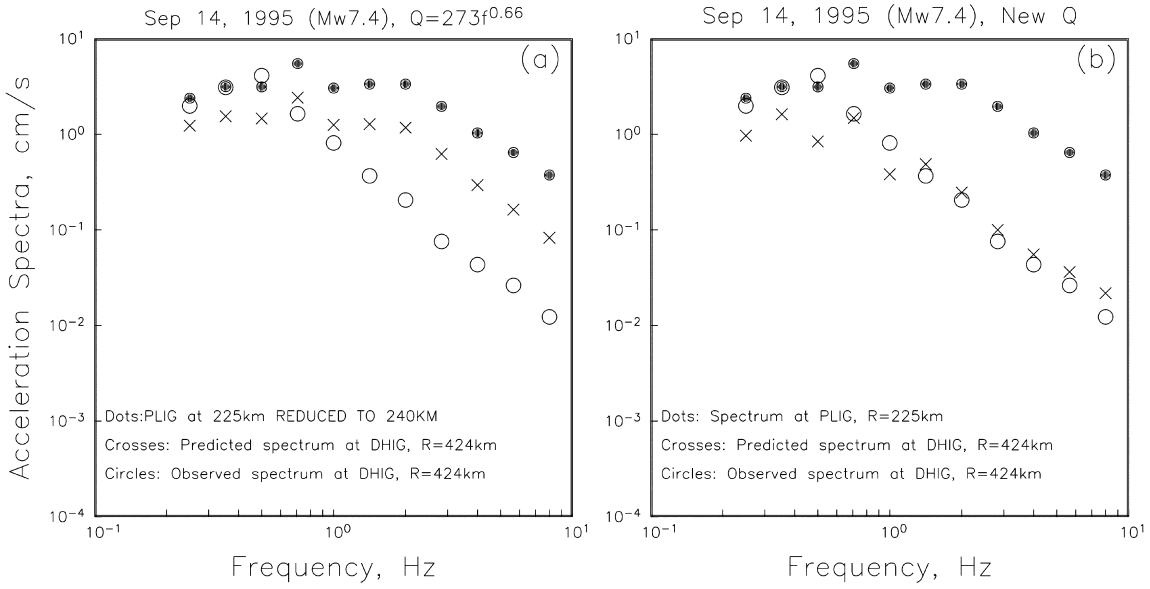

Figure 6. Comparison of observed and predicted amplitudes at DHIG during the Copala 1995 earthquake (M_w 7.4). Observed spectral amplitudes at PLIG and Q of *Lg* waves of the MVB were used to predict the spectrum at DHIG. (a) Prediction assuming Q of the MVB equals that of the forearc (i.e., $Q = 273f^{0.66}$). (b) Prediction based on Q of the MVB obtained in this study.

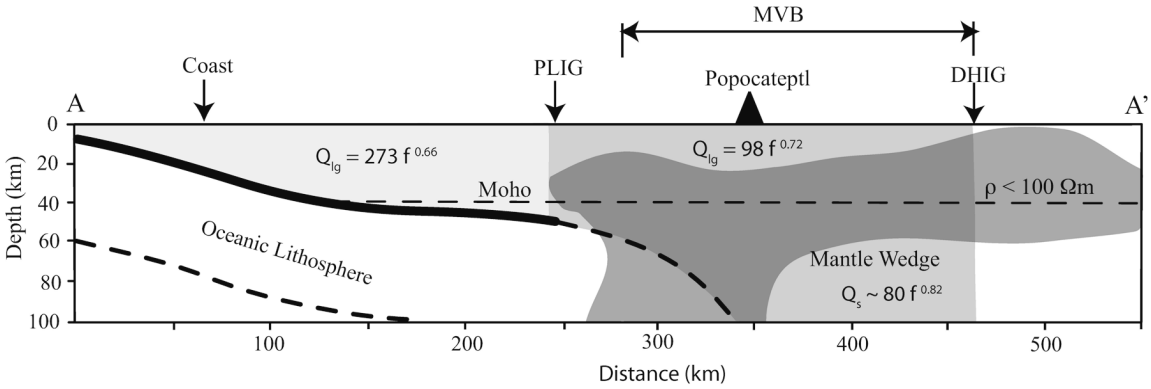

Figure 7. A cross section along AA′ (Fig. 1). The plate interface geometry, modified from Singh and Pardo (1993) and Pardo and Suarez (1995), is shown by a thick line if constrained by hypocenters, otherwise by a dashed line. Moho depth is modified from Campillo *et al.* (1996) and Iglesias *et al.* (2001). Q of the forearc region, the MVB, and the mantle wedge are taken from Ordaz and Singh (1992), this study, and Singh *et al.* (2006), respectively. Q of S waves in the subducting oceanic lithosphere may be about the same as the Q of Lg waves in the forearc (Garcia *et al.*, 2004). Region of low resistivity (<100 Ωm), shown by darkly shaded area (Jödicke *et al.*, 2006), roughly, coincides with low Q of MVB.

scribed by $1/R^{1/2}$. Because our assumptions are reasonable and the method is straightforward, we consider our estimate of $Q^{-1}(f)$ of Lg waves in the central MVB to be reliable.

Comparison with Previous Results

Figure 5 compares $Q^{-1}(f)$ of central MVB obtained here with those reported in earlier studies. With one exception, the new $Q^{-1}(f)$ is higher (i.e., the attenuation of seismic waves in the MVB is greater) than previously reported. The exception is $Q^{-1}(f)$ obtained by Ortega and Qunitanar (2005) which is similar to the one reported here (Fig. 5). In view of the differences in the source characteristics and location of the earthquakes, the data and methodology used in the analysis, and the site characteristics of the recording stations, this similarity may only be fortuitous. Note that our estimate of $Q(f)$ is for a 200-km-wide zone of the MVB. $Q(f)$ of the southern MVB, which is presently active, is probably much lower. For example, Q of S wave at 1 Hz below the active Popocatepetl volcano (Shapiro *et al.*, 2000) is smaller than the present estimate (Fig. 5).

Implications for Seismic Engineering

The estimate of $Q(f)$ across the central MVB can be used to predict the spectrum of Lg waves at the northern end of the MVB from future coastal earthquakes. An example is provided by the Copala earthquake of 1995 (M_w 7.4). The location of the earthquake is shown in Figure 1. This earthquake was recorded at PLIG and by a portable broadband seismograph at DHIG. The observed spectrum at PLIG and $Q(f)$ of Lg waves of the MVB, obtained in this study, were used to predict the spectrum at DHIG. As shown in Figure 6, the agreement between observed and predicted spectral amplitudes at DHIG for $f > 0.5$ Hz is excellent. This demonstrates that our estimate of $Q(f)$ across the central MVB has practical engineering application; once the source spectrum of a coastal earthquake is specified, a reliable estimate of the Fourier spectrum of the ground motion to the north of the MVB and, via random vibration theory, other ground motion parameters may be obtained.

Tectonic Implications

We note that $Q(f)$ of Lg waves in the MVB is significantly lower than in the forearc region reported by Ordaz and Singh (1992) (Fig. 5). Similar observations have been made in northeastern Japan (see, e.g., Takanami *et al.*, 2000; Tsumura *et al.*, 2000; Yoshimoto *et al.*, 2006). Low $Q(f)$ is probably due to heating and partial melting of crustal material, presence of fluids, and enhanced scattering from heterogeneities and fractures resulting from active tectonics of the volcanic zone.

Figure 7 illustrates a section along AA′ of Figure 1. It shows the geometry of the Benioff zone and the distribution of $Q(f)$. It also outlines the region of low resistivity (<100 Ωm) reported by Jödicke *et al.* (2006) from the inversion of magnetotelluric data. Roughly, the region of low Q below the MVB also has low resistivity. The existence of the zone of low resistivity has been attributed to the presence of subduction-related fluids and partial melts (Jödicke *et al.*, 2006), factors that also gives rise to low $Q(f)$ (see, e.g., Mitchell, 1995). It seems, however, that that low $Q(f)$ is not always associated with low resistivity, for ex-

ample, the upper crust of the MVB (Fig. 7). Perhaps fluids and partial melts are less abundant in the upper crust so that the resistivity is high even though $Q(f)$ is low, perhaps because of intense scattering caused by faults and fractures.

Conclusions

1. We have used recordings of shallow earthquakes along the Pacific coast of Mexico at a pair of broadband stations to determine $Q(f)$ of *Lg* waves of MVB. The stations are located on limestone and straddle the central MVB. Because our estimate, $Q(f) = 98f^{0.72}$, is based on reasonable assumptions and straightforward analysis, we believe that it provides a reliable average for the central MVB. This estimate is roughly the same as that reported by Ortega and Quintanar (2005) but is lower than all other previous ones. It is much lower than $Q(f) = 273f^{0.66}$ for the forearc region. Low Q of the central MVB is most probably due to heating and partial melting of crustal material, presence of fluids, and enhanced scattering caused by fractures and faults in this tectonically active region.
2. Q of *Lg* waves across MVB provides one of the needed parameters to estimate ground-motion parameters to the north of the MVB from future coastal earthquakes via random vibration theory.
3. Q seems to correlate with resistivity; the MVB has lower Q and lower resistivity as compared with the forearc region. This correlation is expected since low resistivity below the MVB is probably a consequence of subduction-related fluids and partial melts. These are also some of the factors that give rise to low Q.

Acknowledgments

We are grateful to M. Campillo, T. Furumura, and two anonymous referees for their thoughtful comments. We thank the technicians of the National Seismological Service (SSN) of the Instituto de Geofisica, Universidad Nacional Autónoma de México who, often under rather adverse circumstances, maintain the broadband seismic network. The research was supported in part by DGAPA, UNAM project IN114305, and CONACyT project 42671-T.

References

Campillo, M., S. K. Singh, N. Shapiro, J. Pacheco, and R. B. Hermann (1996). Crustal structure of the Mexican volcanic belt, based on group velocity dispersion, *Geofis. Int.* **35,** 361–370.

Canas, J. A. (1986). Estudio de factor inelástico Q de la coda de los terremotos correspondientes a las regiones central y oriental del eje volcánico de México, *Geofis. Int.* **25,** 503–520.

Demant, A. (1981). L'Axe Néo-Volcanique Transmexicain, Etude volcanologique et pétrographique. Signification géodynamique, *Thése de doctorat*, Université de droit, d'économie et des sciences d'Aix'Marseille, Marseille.

Ferrari, L. (2004). Slab detachment control on mafic volcanic pulse and mantle heterogeneities in central Mexico, *Geology* **32,** 77–80.

Figueroa, J. (1987). Isosistas de grandes temblores ocurridos en la república mexicana, Rept. Instituto de Ingeniería, Universidad Nacional Autónoma de México, Mexico, D.F.

García, D., S. K. Singh, M. Herráiz, J. F. Pacheco, and M. Ordaz (2004). Inslab earthquakes of central Mexico: Q, source spectra and stress drop, *Bull. Seism. Soc. Am.* **94,** 789–802.

Global Centroid Moment Tensor (CMT) Project catalog search. www.globalcmt.org/CMTsearch.html (last accessed June 2007).

Iglesias, A., V. M. Cruz-Atienza, N. M. Shapiro, S. K. Singh, and J. F. Pacheco (2001). Crustal structure of south-central Mexico estimated from the inversion of surface-wave dispersion curves using genetic and simulated annealing algorithm, *Geofis. Int.* **40,** 181–190.

Jödicke, H., A. Jording, L. Ferrari, J. Arzate, K. Mezger, and L. Rüpke (2006). Fluid release from the subducted Cocos plate and partial melting of the crust deduced from magnetotelluric studies in Southern Mexico: Implications for the generation of volcanism and subduction dynamics, *J. Geophys. Res.* **111,** B08102, doi 10.1029-2005 JB003739.

Mitchell, B. J. (1995). Anelastic structure and evolution of the continental crust and upper mantle from seismic surface wave attenuation, *Rev. Geophys.* **33,** 441–462.

Ordaz, M., and S. K. Singh (1992). Source spectra and spectral attenuation of seismic waves from Mexican earthquakes, and evidence of amplification in the hill zone of Mexico City, *Bull. Seism. Soc. Am.* **82,** 24–43.

Ortega, R., and L. Quintanar (2005). A study of local magnitude scale in the Basin of Mexico: Mutually consistent estimate of $\log A_0$ and ground motion scaling, *Bull. Seism. Soc. Am.* **95,** 605–613.

Ortega, R., R. B. Herrmann, and L. Quintanar (2003). Earthquake ground-motion scaling in central Mexico, *Bull. Seism. Soc. Am.* **93,** 397–413.

Ottemöller, L., N. M. Shapiro, S. K. Singh, and J. F. Pacheco (2002). Lateral variation of Lg wave propagation in southern Mexico, *J. Geophys. Res.* **107,** no. B1, 2008, 10.1029/2001JB000206.

Pardo, M., and G. Suárez (1995). Shape of the subducted Rivera and Cocos plates in southern Mexico: seismic and tectonic implications, *J. Geophys. Res.* **100,** 12,357–12,373.

Robin, C. (1981). Relations volcanologie-magmatologie-géodynamique: application au passage entre volcanismes alcalin et andésitique dans le sud mexicain, *Thése de doctorat*, Université de Clermont-Ferrand II, Clermont-Ferrand.

Shapiro, N. M., M. Campillo, A. Paul, S. K. Singh, D. Jongmans, and F. J. Sánchez (1997). Surface wave propagation across the Mexican volcanic belt and the origin of the long-period seismic-wave amplification in the Valley of Mexico, *Geophys. J. Int.* **128,** 151–166.

Shapiro, N. M., S. K. Singh, A. Iglesias-Mendoza, V. M. Cruz-Atienza, and J. F. Pacheco (2000). Evidence of low Q below Popocateptl volcano and its implications to seismic hazard in México City, *Geophys. Res. Lett.* **27,** 2753–2756.

Singh, S. K., and M. Pardo (1993). Geometry of the Benioff zone and the state of stress in the overriding plate in central Mexico, *Geophys. Res. Lett.* **20,** 1483–1486.

Singh, S. K., J. Lermo, T. Domínguez, M. Ordaz, J. M. Espinosa, E. Mena, and R. Quaas (1988a). A study of amplification of seismic waves in the Valley of Mexico with respect to a hill zone site (CU), *Earthquake Spectra* **4,** 653–674.

Singh, S. K., E. Mena, and R. Castro (1988b). Some aspects of source characteristics of the 19 September 1985 Michoacan earthquake, and ground motion amplification in and near Mexico City from strong motion data, *Bull. Seism. Soc. Am.* **78,** 451–477.

Singh, S. K., J. F. Pacheco, D. García, and A. Iglesias (2006). An estimate of shear-wave Q of the mantle wedge in Mexico, *Bull. Seism. Soc. Am.* **96,** 176–187.

Singh, S. K., R. Quaas, M. Ordaz, F. Mooser, D. Almora, M. Torres, and R. Vasquez (1995). Is there truly a "hard" rock site in the Valley of Mexico? *Geophys. Res. Lett.* **22,** 481–484.

Takanami, T., I. Selwyn Sacks, and A. Hasegawa (2000). Attenuation structure beneath the volcanic front in northeastern Japan from broad-band seismograms, *Phys. Earth Planet. Interiors* **121,** 339–357.

Tsumura, N., S. Matsumoto, S. Horiuchi, and A. Hasegawa (2000). Three-dimensional attenuation structure beneath the northeastern Japan arc estimated from spectra of small earthquakes, *Tectonophysics* **319,** 241–260.

Verma, S. P. (2002). Absence of Cocos plate subduction-related mafic volcanism in southern Mexico: a unique case on Earth? *Geology* **30,** 1095–1098.

Yamamoto, J., L. Quintanar, R. B. Herrmann, and C. Fuentes (1997). Lateral variations of Lg coda Q in southern Mexico, *Pageoph* **149,** 575–599.

Yoshimoto, K., U. Wegler, and M. Korn (2006). A volcanic front as a boundary of seismic-attenuation structures in northeastern Honshu, Japan, *Bull. Seism. Soc. Am.* **96,** 637–646.

Instituto de Geofísica
Ciudad Universitaria, Universidad Nacional Autónoma de México
04510 México D.F., Mexico
(S.K.S., J.F.P.)

Instituto de Ingeniería
Ciudad Universitaria, Universidad Nacional Autónoma de México
04510 México D.F., Mexico
(A.I., M.O.)

Departamento de Geofísica y Meteorología
Facultad de Ciencias Físicas, Universidad Complutense de Madrid (UCM)
Ciudad Universitaria
28040 Madrid, Spain
(D.G.)

Manuscript received 1 August 2006.